European Journal of Pharmaceutics and Biopharmaceutics 84 (2013) 275–287

Contents lists available at SciVerse ScienceDirect

European Journal of Pharmaceutics and Biopharmaceutics

journal homepage: www.elsevier.com/locate/ejpb

Research paper

Flotillin-involved uptake of silica nanoparticles and responses of an alveolar-capillary barrier *in vitro*

Jennifer Kasper [a,*], Maria I Hermanns [b], Christoph Bantz [c], Stefanie Utech [c], Olga Koshkina [d], Michael Maskos [c,d,e], Christoph Brochhausen [a], Christine Pohl [a], Sabine Fuchs [f], Ronald E. Unger [a], C. James Kirkpatrick [a]

[a] *Institute of Pathology, University Medical Centre, Mainz, Germany*
[b] *Institut für klinische Forschung und Entwicklung, ikfe GmbH, Mainz, Germany*
[c] *Institute of Physical Chemistry, Johannes Gutenberg University Mainz, Mainz, Germany*
[d] *Federal Institute for Materials Research and Testing, BAM, Berlin, Germany*
[e] *Institut für Mikrotechnik, Mainz, Germany*
[f] *Experimental Trauma Surgery, University Medical Center Schleswig-Holstein, Kiel, Germany*

ARTICLE INFO

Article history:
Available online 24 November 2012

Keywords:
Silica nanoparticles
Alveolar-capillary barrier
NP uptake
NP-transport
Endocytosis
Flotillin-1/-2-dependent uptake/trafficking

ABSTRACT

Drug and gene delivery via nanoparticles across biological barriers such as the alveolar-capillary barrier of the lung constitutes an interesting and increasingly relevant field in nanomedicine. Nevertheless, potential hazardous effects of nanoparticles (NPs) as well as their cellular and systemic fate should be thoroughly examined. Hence, this study was designed to evaluate the effects of amorphous silica NPs (Sicastar) and (poly)organosiloxane NPs (AmOrSil) on the viability and the inflammatory response as well as on the cellular uptake mechanisms and fate in cells of the alveolar barrier. For this purpose, the alveolar epithelial cell line (NCI H441) and microvascular endothelial cell line (ISO-HAS-1) were used in an experimental set up resembling the alveolar-capillary barrier of the lung. In terms of IL-8 and sICAM Sicastar resulted in harmful effects at higher concentrations (60 μg/ml) in conventional monocultures but not in the coculture, whereas AmOrSil showed no significant effects. Immunofluorescence counterstaining of endosomal structures in NP-incubated cells showed no evidence for a clathrin- or caveolae-mediated uptake mechanism. However, NPs were enclosed in flotillin-1 and -2 marked vesicles in both cell types. Flotillins appear to play a role in cellular uptake or trafficking mechanisms of NPs and are discussed as indicators for clathrin- or caveolae-independent uptake mechanisms. In addition, we examined the transport of NPs across this *in vitro* model of the alveolar-capillary barrier forming a tight barrier with a transepithelial electrical resistance of 560 ± 8 Ω cm^2. H441 in coculture with endothelial cells took up much less NPs compared to monocultures. Moreover, coculturing prevented the transport of NP from the epithelial compartment to the endothelial layer on the bottom of the filter insert. This supports the relevance of coculture models, which favour a differentiated and polarised epithelial layer as *in vitro* test systems for nanoparticle uptake.

1. Background

Nanoparticles (NPs) play a decisive role in industrial applications on the one hand, and on the other hand, NPs are gaining in interest for biomedical research (drug and gene delivery) [1]. Regarding an entry of NPs via inhalation, the alveolar region of the lung with a surface area of 100–140 m^2 make it an interesting target for drug and gene delivery, but at the same time, the lung represents a significant portal of entry for harmful nanomaterials. Inhaled silica nanoparticles (SNPs), for example, embody a serious health-risk characterised by environmental and occupational lung diseases (silicosis) [2]. It has been proposed that pulmonary release of cytokines and mediators into the circulation, that are triggered by inhaled NPs, cause extrapulmonary effects [3]. Epidemiological studies revealed that particulate air pollution (PM_{10}: Particulate matter <10 μm) increased the frequency of cardiac diseases [4,5]. However, plausible explanations from the biological perspective are still lacking. It is also suggested that the resulting systemic effects are caused by an excess of inhaled PM_{10} that migrate into

Abbreviations: AmOrSil, amorphous organosiloxane particles; ANOVA, analysis of variance; aSNP, amorphous silica nanoparticles; CatD, cathepsin-D; Cav, caveolin-1; CC, coculture; CHC, clathrin heavy chain; DLS, dynamic light scattering; EC, endothelial cells; EEA1, early endosome antigen 1; Flot1, flotillin-1; Flot2, flotillin-2; IF, immunofluorescence; M6PR, mannose-6-phosphate receptor; MC, conventional monoculture; NP, nanoparticle; Pen/Strep, penicillin/streptomycin; PM10, particulate material with a diameter <10 μm; RFU, relative fluorescent unit; SNPs, silica nanoparticles; TEM, transmission electron microscopy.

* Corresponding author. University Medical Centre, Institute of Pathology, Mainz, Germany. Tel.: +49 (0) 6131 173925; fax: +49 (0) 6131 17534.
E-mail address: kasperj@uni-mainz.de (J. Kasper).

0939-6411
http://dx.doi.org/10.1016/j.ejpb.2012.10.011

the systemic circulation and then translocate to different organs [6,7].

Thus, if a lung application is envisaged, toxic effects and the cellular pathways as well as the further disposition of inhaled NPs need to be addressed to gain more insight concerning the above mentioned hypotheses.

Cytotoxicity and cellular uptake/trafficking of nanoparticles in the lower respiratory tract are still poorly understood. One reason for this is that the alveolar-capillary barrier of the deep lung is difficult to access by *in vivo* studies. Therefore, we have inspected nanoparticle interactions on an *in vitro* coculture model of the alveolar-capillary. This *in vitro* model consists of the epithelial cell line, NCI H441 (with characteristics of type II pneumocytes and Clara cells) and the human microvascular endothelial cell (MEC) line, ISO-HAS-1, which are seeded on opposite sides of a transwell filter membrane. Both cell types in coculture (CC) reach a more differentiated and polarised phenotype than if the cells are kept under conventional monoculture (MC) conditions [8,9]. Therefore, it more closely mimics the *in vivo* situation of the deep lung.

Two silica-based nanoparticles such as Sicastar Red (aSNP: amorphous silica, 30 nm in diameter) and AmOrSil (poly(organosiloxane), ca. 100 nm) have been used. Sicastar rather resembles SNPs that are used for industrial purposes and embodies a cytotoxic NP, which is supposed to evoke inflammatory responses to study cell communication processes in the coculture. Whereas AmOrSil is prospectively envisaged for *in vitro* studies concerning drug and gene delivery and is proposed to be nontoxic. AmOrSil has a magnetic core, which may be useful for therapeutic applications (hyperthermia, magnetic resonance imaging or drug delivery) [10,11].

At first, the cytotoxicity (MTS and LDH) was studied on H441 and ISO-HAS-1 in MC and CC. Subsequently, NP uptake behaviour of the epithelial cells (H441) in CC was compared to the epithelial cells kept in MC by fluorescence intensity measurements. Furthermore, transport of NPs across the NP-exposed epithelial layer with subsequent uptake by the endothelial layer (ISO-HAS-1) on the opposite side of the transwell filter membrane was examined. In addition, NP-exposed cells were immunofluorescently counterstained for endosomal marker proteins such as clathrin heavy chain or caveolin-1 as well as flotillin-1 and -2 to examine specific uptake mechanisms such as clathrin-dependent or caveolae-dependent endocytosis.

Finally, the release of inflammatory mediators (IL-8, sICAM) has been examined after NP exposure to the apical side of the coculture (H441) to study inflammatory responses and cell communication processes between epithelial and endothelial cells. In correlation with the uptake/transport experiments with the coculture, these results provide an approach to the hypothesis concerning indirect (forwarded inflammatory mediators caused by NPs) or direct (translocation of NPs) extrapulmonary effects caused by inhaled nanoparticles.

2. Materials and methods

2.1. Nanoparticle characterisation

2.1.1. AmOrSil

AmOrSil nanoparticles were synthesised and delivered by Stefanie Utech (Department of Physical Chemistry of the Johannes Gutenberg University, Mainz). These NPs are magnetic nanocapsules with magnetic iron oxide particles incorporated into a poly(organosiloxane) network that carries an additional PEO shell. The synthesis of the poly(organosiloxane) core–shell nanoparticles was performed in aqueous dispersion by co-condensation of a mixture of alkyldialkoxysilanes (diethoxydimethylsilane) and alkyltrialkoxysilanes (trimethoxymethylsilane and (chloromethylphenyl) trimethoxysilane, as functional monomers) in the presence of a surfactant. Rhodamine B was covalently incorporated into the entire SiO_x-matrix. Magnetic iron oxide nanoparticles (γ-Fe_2O_3) with an average radius of 3.2 nm were encapsulated during the polycondensation process. Water-solubility was achieved via a grafting-on process, in which linear PEG (poly(ethylene glycol), MW: 1650 g/mol) was covalently attached to the poly(organosiloxane) surface. The magnetic nanocapsules have a primary particle radius of 48.1 nm. Synthesis and characterisation have previously been described by Utech et al. [10,11].

2.1.2. Sicastar Red

Sicastar Red is an amorphous silica nanoparticle (30 nm in size) in aqueous dispersion which contains rhodamin B covalently incorporated into the entire SiO_2-matrix. The manufacturing technique is described by micromod Partikeltechnologie GmbH [12].

The hydrodynamic radii of both Sicastar Red and AmOrSil particles in aqueous solutions (water, phosphate buffered saline (PBS) and serum-free cell culture medium RPMI) were determined via dynamic light scattering (DLS) as previously described for the characterisation of non-fluorescent amorphous silica nanoparticles [9]. The results are shown in Table 1. Both samples show an increased hydrodynamic radius in salt-containing media compared to the primary particle radius (determined by transmission electron microscopy and asymmetrical flow field-flow fractionation, data not shown). In the case of the Sicastar Red, the dispersions destabilized with higher salt contents and the particles partly agglomerate; for the AmOrSil, the increase in size compared to the primary particles is not yet completely understood, but it can probably be explained by loose entanglements of the attached poly(ethylene oxide) molecules. The mean hydrodynamic diameter of both particles is ca. 100 nm (radius: 48.1 nm).

2.1.3. Cell culture

ISO-HAS-1 (human microvascular endothelial cell line [13,14]) and NCI H441 (human lung adenocarcinoma cell line, purchased from ATCC, ATCC-HTB-174, Promochem, Wesel, Germany) were grown in RPMI 1640 supplemented with 10% FCS (foetal calf serum), 1% P/S (Penicillin/Streptomycin). ISO-HAS-1 and H441 were passaged every third day at a dilution of 1:3 until passage 50 and 35, respectively.

2.1.4. Monocultures in experimental procedures

Prior to seeding cells, the 96-well plates (TPP, Switzerland) or eight well μ-slides (ibidi) were coated with 50/300 μl fibronectin for 1 h at 37 °C (5 μg/ml, Roche Diagnostics, Mannheim). The cells were seeded (ISO-HAS-1: 1.6×10^4 cells/well, H441: 3.2×10^4 cells/well) from a confluent culture flask on 96-well plates in RPMI 1640 medium (Gibco) with L-glutamine supplemented with 10% FCS and Pen/Strep (100 U/100 μg/ml) and cultivated at 37 °C, 5% CO_2 for 24 h prior to NP exposure to a confluent cell layer.

Table 1
Hydrodynamic radii of the silica-based nanoparticles (SicaStar Red and AmorSil) in different media obtained via dynamic light scattering.

Medium	H_2O	PBS buffer	Cell medium
AmorSil			
$\langle R_h \rangle_z$ (nm)	52.9	47.9	48.1
μ_2	0.17	0.09	0.11
Sicastar Red			
$\langle R_h \rangle_z$ (nm)	12.6	66.2	58.1
μ_2	0.10	0.16	0.17

2.1.5. The coculture model of the alveolar-capillary barrier of the distal lung

The coculture procedure was performed as described by Hermanns et al. [15] with some alterations. HTS 24-Transwell® filters (polycarbonate, 0.4 μm pore size; Costar, Wiesbaden, Germany) were coated with rat tail collagen type-I (12.12 μg/cm^2, BD Biosciences, Heidelberg, Germany). ISO-HAS-1 cells (1.6×10^4/well ≙ 5×10^4/cm^2) were seeded on the lower surface of the inverted filter membrane. After 2 h of adhesion at 37 °C and 5% CO_2, H441 (8.4×10^3/well ≙ 2×10^4/cm^2) were placed on the top side of the membrane. The cells were cultured for about 10 days in RPMI 1640 medium with L-glutamine supplemented with 5% FCS, Pen/Strep (100 U/100 μg/ml). From day 3 of cultivation, the H441 were treated with dexamethasone (1 μM). As a control, monocultures of H441 or ISO-HAS-1 were seeded on transwells and kept under the same culture conditions as described for the cocultures. From day 10 on, they show trans-bilayer electrical resistance (TER) values that average 560 ± 6 Ω cm^2.

2.1.6. Nanoparticle application on cell culture

To prevent nanoparticle aggregation, predilutions of the NP-dispersions were prepared in pure water (Braun ad injectabilia, Braun Melsungen AG, Melsungen). Due to nanoparticle aggregation in serum-containing medium, serum-free medium was used during 4 h exposure. All dilutions were applied 1:10 in serum-free medium to the cells (96er well and transwells: 10 μl NP-dispersion + 90 μl serum-free medium and ibidi wells: 30 μl NP-dispersion + 270 μl serum-free medium). For colocalisation studies, an exposure time of 20 min, 4 h and 4 h/20 h (after 4 h incubation cells were washed twice with serum-free medium and further cultivated for 20 h period with fresh serum-containing medium) was chosen. For the coculture, NPs were exclusively applied to the apical side of the H441 layer on top of the transwells.

For a permanent 48 h exposure on the coculture, NPs were apically applied (H441) in serum-free medium for 4 h as described above. After 4 h, serum (2.5% end concentration) and dexamethasone (1 μM) were added in order to maintain stable barrier properties (transepithelial electrical resistance TER) over this long incubation period.

2.1.7. Cytotoxicity

Cell viability was determined by measuring mitochondrial activity using the CellTiter 96® AQueous One Solution Cell Proliferation Assay (MTS, Promega, G3582). After 4 h of nanoparticle exposure, cells were washed twice with PBS to remove nanoparticle remnants, which may cause interferences with the MTS reagent. The MTS reagent (MTS stock solution mixed with medium in a ratio of 1:10) was added to the cell layer. The OD was measured at 492 nm after 45 min incubation at 37 °C.

2.1.8. Membrane integrity

To determine membrane disruption of nanoparticle-exposed H441 and ISO-HAS-1, lactate dehydrogenase (LDH) release into the supernatant of the cells was measured using LDH CytoTox 96® Non-Radioactive Cytotoxicity Assay (Promega, G1780) according to the manufacturer's recommendations.

2.1.9. Inflammatory responses

The supernatant of nanoparticle-exposed H441 and ISO-HAS-1 in monoculture as well as coculture (upper and lower compartment) was collected to determine IL-8 and soluble sICAM release via ELISA (DuoSet R&D, DY208) according to the manufacturer's recommendations. As positive control, cells were incubated with TNF-α (300 U/ml ≅ 0.732 g/ml) or lipopolysaccharide from *Escherichia coli* (LPS, 1 μg/ml).

2.1.10. Trans-bilayer electrical resistance measurements

To determine the functional efficiency of an intact barrier *in vitro*, the transepithelial electrical resistance (TER) was measured with an EVOM volt ohm meter (World Precision Instruments, Berlin, Germany) equipped with a STX-2 chopstick electrode. HTS 24-Transwell® filter membranes without cells coated with rat tail collagen type-I were measured and set as blank (approximately 110 Ω). Barrier resistance readings (Ω) obtained for each well individually and after subtracting the resistance of the blank filter membrane were multiplied by the membrane area (0.33 cm^2) to give Ω cm^2. In the experiments showing a time-dependent effect of SNP exposure, the TER is expressed as% of t_0 (TER value before SNP exposure).

2.1.11. Immunofluorescence (IF) for endosomal marker proteins

Immunofluorescence (IF) for endosomal marker proteins was performed to label endocytic marker proteins such as clathrin heavy chain (chc: BD, 610499) or caveolin-1 (cav: SantaCruz, sc-894) as well as flotillin-1 and -2 (BD, 610821, BD, 610383). After nanoparticle exposure, cells were fixed with methanol/ethanol in a ratio of 2:1 for 15 min at room temperature. After fixation, cells were incubated with primary antibody diluted in 1% PBSA over night at 4 °C. After three washing steps with PBS, cells were incubated with secondary antibody (Alexa Fluor 488, Invitrogen, A11029) for 1 h at room temperature. Subsequently, cells were washed three times with PBS, and nuclei were stained with Hoechst 33342 (Molecular Probes) for 5 min and washed three times. Finally, cut transwell filters were mounted with Fluoromount-G™ (Southern Biotech, Birmingham), and ibidi μ-slides were mounted with ibidi mounting medium (ibidi, Martinsried).

2.1.12. Nanoparticle uptake behaviour of H441 in conventional mono- and coculture conditions

To draw comparisons concerning uptake behaviour and quantification between H441 in conventional monoculture and H441 kept under coculture conditions, cells were incubated with fluorescently labelled NPs (Sicastar Red: 6 μg/ml, AmorSil: 300 μg/ml) and observed with a fluorescence microscope (DeltaVision, Applied Precision). To allow comparisons, the exposure time and intensity scale were adjusted for each sample to be compared. Subsequently, mean fluorescence intensity was measured via Fiji (http://pacific.mpi-cbg.de) and depicted as relative fluorescent unit (RFU) related to the untreated control (*x*-fold of untreated control).

To evaluate putative transcytosis events, H441 (in coculture with ISO-HAS-1) were incubated with Sicastar Red (60 μg/ml), AmorSil (300 μg/ml) for 48 h. Subsequently, ISO-HAS-1 were checked for internalised NPs by direct observations of images taken with a fluorescence microscope (DeltaVision, Applied Precision). Due to a high autofluorescence of the polycarbonate filter, a quantification of the fluorescent signal by measuring the intensity via Fiji was not suitable.

2.1.13. Electron microscopy

For transmission electron microscopy (TEM), H441 were seeded on fibronectin-coated Thermanox™ coverslips (Nunc #174969, Wiesbaden, Germany) and exposed to AmOrSil for 4 h and further 20 h cultivation in fresh serum-containing medium. Subsequently, cells were fixed in 2.5% glutaraldehyde in cacodylate buffer (pH 7.2) for 30 min then fixed in 1% OsO4 for 2 h and dehydrated in graded ethanol. The coverslips with cells were carried through propylene oxide as an intermedium; then, the samples were embedded in agar 100 resin (PLANO, Wetzlar, Germany) and submitted to polymerisation at 60 °C for 48 h. Ultrathin sections were cut with an ultramicrotome (Leica, Bensheim, Germany). The sections were then placed onto copper grids, and ultrastructural analysis

was performed with a transmission electron microscope (model EM 410; Philips, Eindhoven, Netherlands).

2.1.14. Statistical analysis

From several independent measurements, means and standard deviations were calculated. Data are shown as mean ± SD from at least three separate experiments. Testing for significant differences between means was carried out using one-way ANOVA and Dunnett's Multiple Comparison test at a probability of error of 5% (*), 1% (**) and 0.1% (***).

3. Results

3.1. Cytotoxicity of conventional monocultures after nanoparticle exposure

Two silica-based NPs were investigated: 1. Sicastar Red (amorphous silica; primary particles ca. 30 nm in diameter) and 2. AmOrSil [(poly(organosiloxane) with a shell of poly(ethylene oxide), PEO, to ensure particle solubility in water; primary particles ca. 60 nm in diameter)].

Fig. 1A depicts the viability (MTS assay) and membrane integrity (LDH assay) of the lung epithelial cell line H441 and the microvascular endothelial cell line ISO-HAS-1 cultured in conventional monocultures (MC) after exposure to Sicastar Red and AmOrSil for 4 h in serum-free medium. According to MTS, H441 showed a significantly reduced viability at high concentrations of Sicastar Red (100 μg/ml: 14 ± 12%; 300 μg/ml: 60 ± 12% compared to untreated control uc), whereas AmOrSil did not have any effect (e.g. 300 μg/ml: 109 ± 12% compared to uc). Similar observations have been made for the microvascular endothelial cell line ISO-HAS-1 with Sicastar Red (300 μg/ml: 36 ± 18% and 100 μg/ml: 34 ± 4% of uc) as well as AmOrSil (300 μg/ml 111 ± 15% of uc). Sicastar Red did not cause a significant decrease in the mitochondrial activity at 60 μg/ml for both cell types (H441: 98 ± 15% and ISO-HAS-1: 99 ± 12% of uc). With respect to viability, similar effects were obtained for the membrane integrity after NP exposure. H441 showed a significant release of LDH after 4 h exposure to Sicastar Red (300 μg/ml: 90 ± 7.5%, 100 μg/ml: 70 ± 13.6%, 60 μg/ml: 46 ± 22% of lysis control lc), whereas 6 μg/ml Sicastar Red did not show any toxic effects (14.2 ± 12% of lc). Similar to H441, ISO-HAS-1 also displayed a high LDH release at high concentrations (300 μg/ml: 77 ± 7.5%, 100 μg/ml: 57 ± 18% of lc) but not at 60 μg/ml (12 ± 5% of lc). AmOrSil did not cause a change in membrane integrity even at high concentrations of 300 μg/ml in H441 or ISO-HAS-1 (H441: 13 ± 11% and ISO-HAS-1: 4 ± 2.8% of lc).

3.2. Cytotoxicity of Sicastar Red exposed to H441 in coculture with ISO-HAS-1, comparison to conventional monocultures

According to Fig. 1B, LDH release into the apical compartment (H441) of the coculture (CC) was firstly detected at a concentration of 100 μg/ml Sicastar Red (30 ± 5.6% of lysis control, 2-fold of untreated control uc), but to a lower extent as observed for the H441 in MC (57 ± 18% of lc). The LDH release of the H441 in CC further increased with increasing concentrations (300 μg/ml: 49.3 ± 12.4% of lc), which is also lower compared to the MC (90 ± 7.5% of lc). A concentration of 60 μg did not yield higher LDH levels (10.4 ± 2.5% of lc) on the contrary to the MC (46 ± 22% of lc). Thus, the H441 in CC appear to have more intact membrane integrity after NP exposure compared to H441 under MC conditions.

High concentrations of Sicastar Red (300 μg/ml) exhibited minimal assay interferences (assay reagent in cell culture medium with NPs without cells), which was negligible compared to the respective lysis control (H441: 0.95 ± 0.34% and ISO-HAS-1: 4.4 ± 1.6% of lc).

3.3. Inflammatory responses of H441 and ISO-HAS-1 in conventional monoculture after exposure to Sicastar Red and AmOrSil

After 4 h NP exposure, the NP suspension was removed, and the cells were cultured for a further 20 h period to examine IL-8 and soluble sICAM release after NP exposure. Corresponding to the MTS and LDH assay, AmOrSil did not result in any toxic effects on H441 and ISO-HAS-1 concerning IL-8 and sICAM (Fig. 1C). By contrast, Sicastar Red resulted in an IL-8 release in both cell types (H441 and ISO-HAS-1) at 60 μg/ml (H441: 2.1 ± 0.22% and ISO-HAS-1: 2.3 ± 0.1% of uc). Due to the high cytotoxic effects and cell death, which was also observed in the MTS and LDH assay, lower IL-8 levels were measured at higher NP concentrations (100 and 300 μg/ml) compared to 60 μg/ml in both cell types. A significant sICAM release was also observed for Sicastar Red at a concentration of 60 μg/ml (H441: 1.8 ± 0.14% and ISO-HAS-1: 1.6 ± 02% of uc). With increasing concentrations (100 and 300 μg/ml), the sICAM level still remained significantly high for H441 (100 μg/ml: 1.3 ± 0.17%, 300 μg/ml: 1.5 ± 0.3% of uc) and was further augmented for ISO-HAS-1 (100 μg/ml: 1.8 ± 0.32%, 300 μg/ml: 2.6 ± 0.4% of uc).

3.4. Examination of endosomal uptake routes of NPs under conventional monoculture conditions

Colocalisation of NPs with endosomal marker proteins belonging to the clathrin-mediated (clathrin heavy chain) or caveolae-mediated (caveolin-1) endocytosis pathways were performed in H441 and ISO-HAS-1 by means of immunofluorescence staining procedures (Fig. 2, only Sicastar Red is depicted, AmOrSil yielded similar results). Neither Sicastar Red nor AmOrSil exhibited an uptake in such organelles after 20 min, 4 h or 4 h incubation followed by further cultivation for 20 h in fresh serum-containing media. Thus, an early endosomal uptake via this method could not be identified at the three time points investigated. However, after 4 h incubation followed by 20 h of further cultivation, the fluorescence signals of both NPs were clearly colocalised with flotillin-1 and -2 signals in H441 and ISO-HAS-1 (Fig. 3). The NPs were clearly enclosed by flotillin-1 and -2 containing vesicles. In ISO-HAS-1, colocalisation of NPs with flotillin-1/2 was already observed after 4 h, indicating a faster uptake mechanism in these cells (data not shown).

3.5. Visualisation of internalised AmOrSil in H441 cells in conventional monoculture via TEM (transmission electron microscopy)

TEM was used to define at higher magnification the cellular uptake of AmOrSil in endosomes of H441 (Fig. 4). The iron oxide core and its poly(organosiloxane) shell were clearly visible, and the NPs were incorporated into endosomal structures. Sicastar Red NPs were not visible via TEM due to its low electron density, which resulted in a low contrast. Thus, this method was not applicable to associate these NPs to a particular subcellular compartment.

3.6. Quantification of nanoparticle uptake, comparison of H441 under conventional mono- and coculture conditions

Nanoparticle (Sicastar Red and AmOrSil) uptake behaviour of the epithelial cells was determined and compared for H441 under MC and CC conditions. Fig. 5A depicts the quantification of internalised fluorescence-labelled NPs (Sicastar Red: 6 μg/ml, AmOrSil: 300 μg/ml) in H441 for 4 h with further 20 h cultivation in MC and CC (with ISO-HAS-1). Concentrations were chosen to obtain

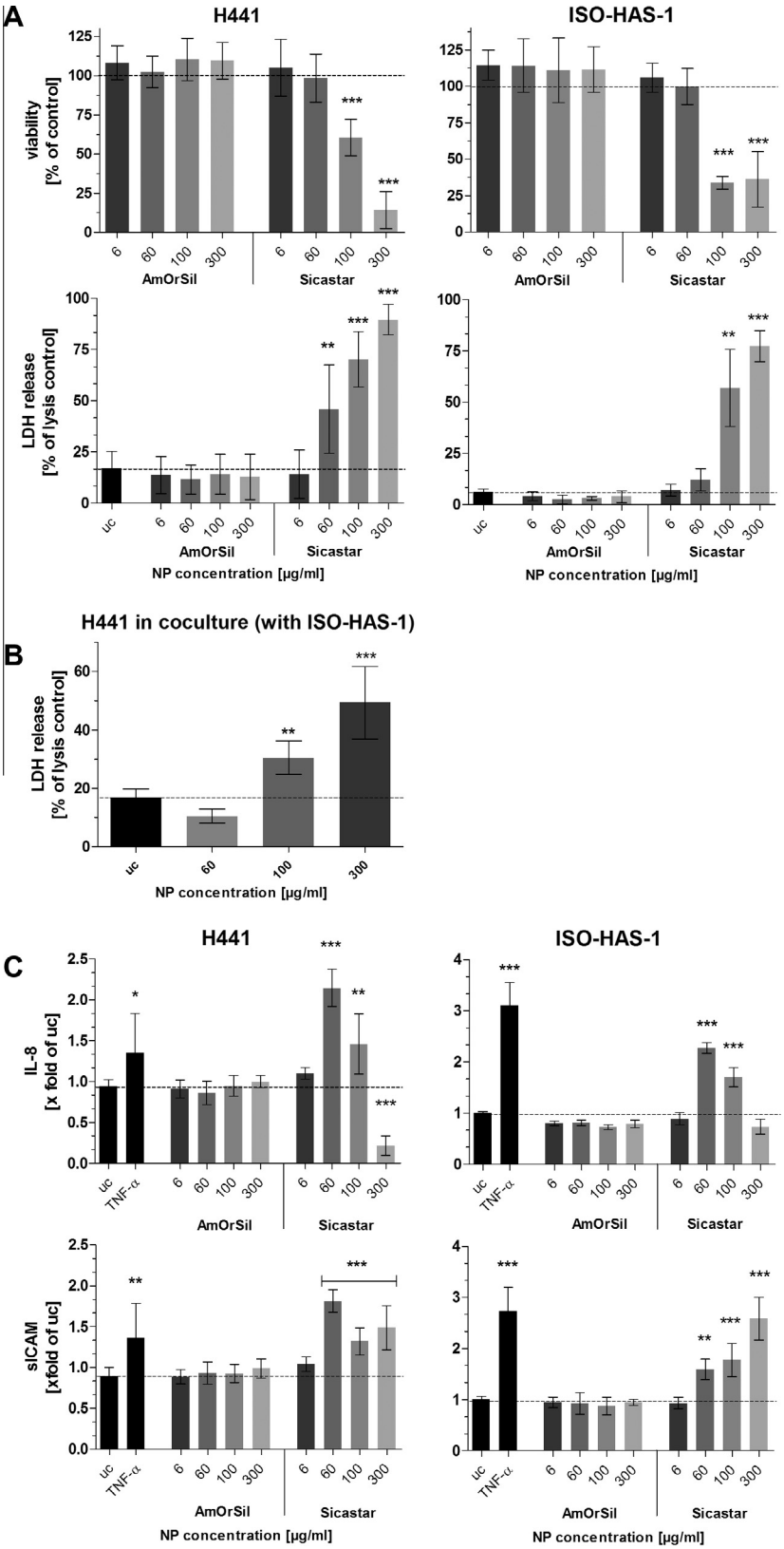

Fig. 1. (A) Exposure of H441 and ISO-HAS-1 in conventional monoculture to Sicastar Red and AmOrSil (6–300 µg/ml),viability (MTS assay) and lactate dehydrogenase release (LDH) of H441 and ISO-HAS-1 following treatment with NPs for 4 h was conducted. (B) LDH release of H441 in coculture with ISO-HAS-1 (upper well is depicted) exposed to Sicastar Red for 4 h. (C) Measurement of inflammatory mediators (IL-8, sICAM) in the supernatant of NP-exposed H441 and ISOHAS-1 in conventional monoculture for 4 h with further 20 h cultivation in serum-containing medium without NPs. Uc: untreated control, TNF-α (300 U/ml). Data are depicted as means ± SD of two independent experiments with $n = 3$ samples for each treatment. For statistical analysis one-way ANOVA with Dunett's post test was applied. $^{*}P < 0.05$, $^{**}P < 0.01$ and $^{***}P < 0.001$ compared to the untreated control (uc).

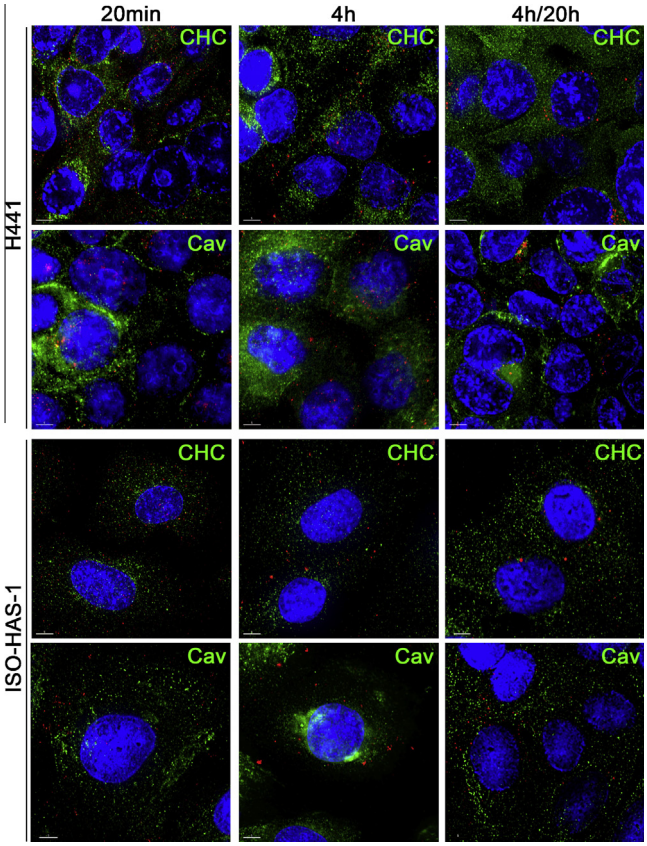

Fig. 2. Incubation of H441and ISO-HAS-1 in conventional monoculture with Sicastar Red (6 μg/ml) for 20 min, 4 h and 4 h with subsequent removal of NPs and culturing for further 20 h in fresh serum-containing medium (red signal). Green signal: Immunofluorescent staining for clathrin heavy chain (CHC) and caveolin-1 (Cav) containing vesicles. Nuclei are stained with Hoechst 33342 (blue). Bar: 5 μm.

adequate fluorescence intensities in order to compare mono- and cocultures.

A significant increase in fluorescence intensity was observed for NP-incubated H441 in MC for both NPs (Fig. 5A: Sicastar Red: 1.5 ± 0.5-fold of uc and AmOrSil: 2.7 ± 0.3-fold of uc). For H441 in CC, however, an uptake via fluorescence intensity measurement could not be detected.

3.7. Visualisation of internalised nanoparticles: comparison of H441 in conventional monoculture and coculture

Based on the visual examination of the microscopic image (Fig. 5B), the uptake of both NP types in H441 in CC appeared extremely low compared to the MC. In Fig. 5C, an elevation of the NP-concentration and exposure time revealed an increased uptake of Sicastar Red (60 μg/ml, 48 h) in H441 in CC. However, an increased uptake of AmOrSil (300 μg/ml, 48 h) could not be verified.

3.8. Examination of endosomal uptake routes of NPs in H441 under coculture conditions

The same exposure times and staining procedures as described above (see Fig. 2) were carried out with H441 grown in CC with ISO-HAS-1 to determine if differences in nanoparticle uptake or trafficking behaviour from H441 under different culture conditions compared to the MC occurred. Although the monoculture of H441 showed fluorescent signals inside the cells after only 4 h of incubation, this time period yielded no uptake in H441 in CC with both NP types as detectable by fluorescence microscopy (data not shown).

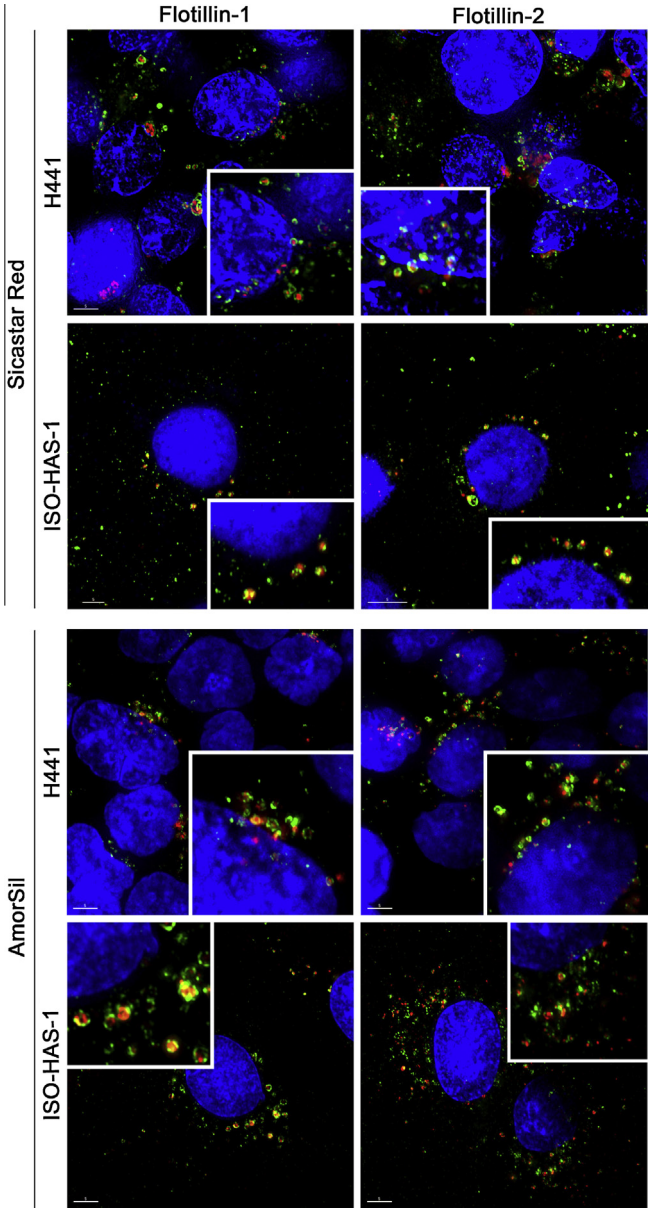

Fig. 3. Uptake studies of immunofluorescence stained vesicles of H441 and ISO-HAS-1 kept in conventional monoculture and exposed to Sicastar Red (6 μg/ml) and AmOrSil (100 μg/ml) for 4 h and further 20 h cultivation (red signal). A clear incorporation of NPs in flotillin-1- and -2-containing vesicles (green signal) could be detected. Nuclei are stained using Hoechst 33342 (blue), scale bar: 5 μm.

Similar to the findings in the MC, no clear uptake in early endosomes (clathrin heavy chain, caveolin-1 and other markers) was detected in the CC at all time points chosen (4 h and 4 h followed by 20 h cultivation in fresh medium without NPs). Accumulation of Sicastar Red in flotillin-1- and -2-bearing vesicles occurred after 20 h following the 4 h incubation period (Fig. 6) similar to that observed in MC. AmOrSil however, did not show any colocalisation with flotillin-1 and 2 (data not shown).

3.9. Evaluation of a transport of NPs across the apically exposed (epithelial side) coculture via fluorescence microscopy

Fig. 7 (left column) shows exposure of ISO-HAS-1 in MC to NPs as it was applied for the colocalisation studies (Sicastar Red 6 μg/ml and AmOrSil: 300 μg/ml, 4 h with 20 h cultivation in

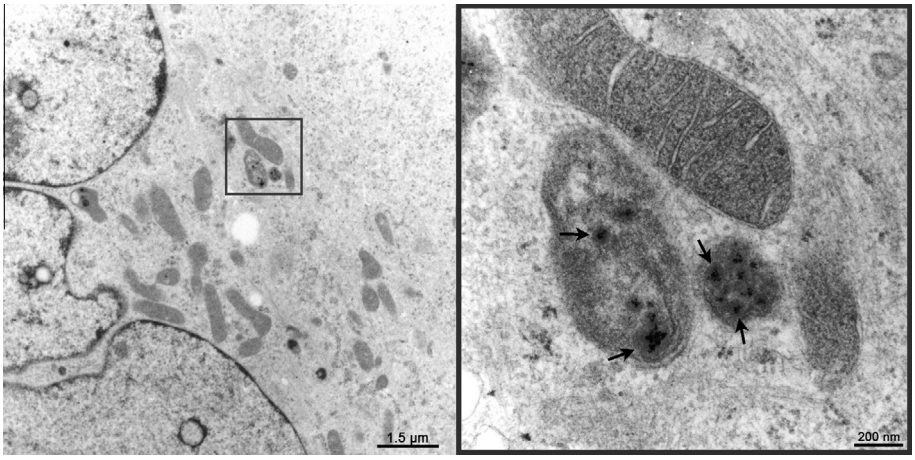

Fig. 4. Transmission electron microscopical images of H441 in conventional monoculture exposed to AmOrSil for 4 h and further 20 h cultivation in fresh serum-containing medium. The iron oxide core with its poly(organosiloxane) shell is clearly visible and incorporated in endosomal structures.

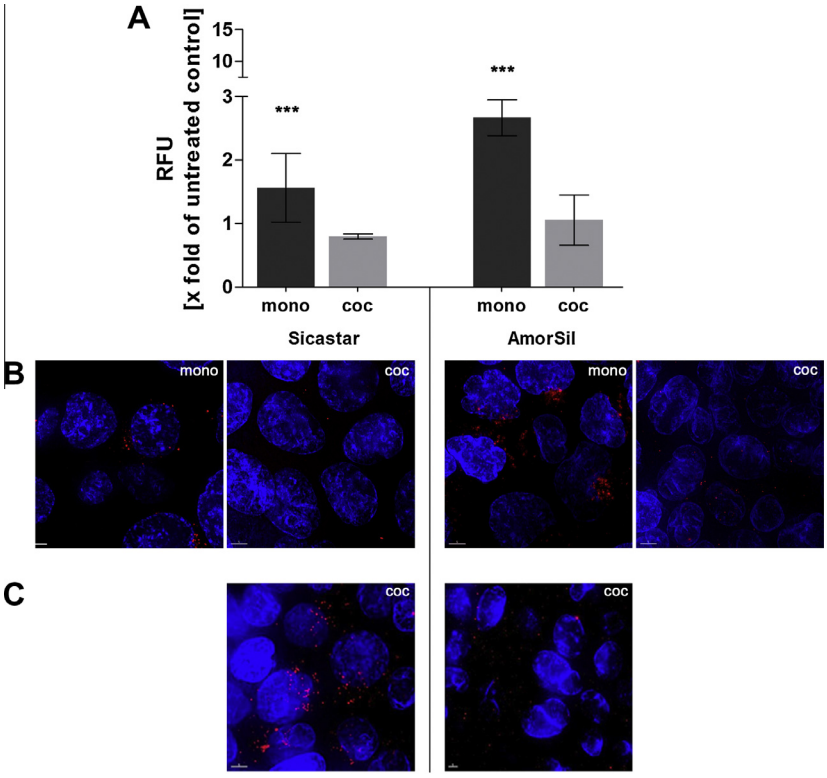

Fig. 5. Comparison of NP uptake behaviour in H441 under different culture conditions (mono: conventional monoculture, coc: differentiated coculture with ISO-HAS-1). Images were taken by means of a fluorescence microscope (DeltaVision, Applied Precision), (A) Incubation with Sicastar Red (6 µg/ml) and AmOrSil (300 µg/ml) for 4 h with further 20 cultivation in serum-containing medium without NPs. Intensity scales were aligned for untreated and treated samples and mean fluorescence intensity was measured via Fiji (http://pacific.mpi-cbg.de). RFU = relative fluorescent unit. Data are depicted as means ± SD from nine images. For statistical analysis the unpaired *t*-test was chosen ($^{*}P < 0.05$, $^{**}P < 0.01$ and $^{***}P < 0.001$ compared to the untreated control). (B) Images: Sicastar Red and AmOrSil (red signal), incubation procedure as described for A. (C) 48 h permanent incubation of Sicastar Red (60 µg/ml)and AmOrSil (300 µg/ml) to H441 in coculture with ISO-HAS-1: uptake for Sicastar Red increased, whereat uptake for AmOrSil remains lower. Nuclei are stained using Hoechst 33342 (blue), scale bar: 5 µm.

serum-containing medium without NPs. A detectable uptake could be verified with direct exposure to NPs for the MC. To evaluate the transport of NPs across the NP-exposed epithelial layer of the CC, the endothelial layer (ISO-HAS-1) on the lower surface was examined for NPs. For this purpose, NPs (Sicastar Red: 60 µg/ml, AmorSil: 300 µg/ml) were continuously applied on the apical side (on the epithelial monolayer of H441) for 48 h. As a control ISO-HAS-1 was seeded on the lower surface of the transwell filter membrane and cultured for 10 days with subsequent indirect (apical) NP-application without H441 on the top (Fig. 7, middle column). A cellular uptake of both NPs could be detected in the ISO-HAS-1 transwell-monoculture. However, compared to the conventional monoculture MC, a lower amount of NPs was taken up. These findings verify that the coculture model system was functional and particles that were applied apically (on top of the filter membrane) and able to diffuse through the collagen-1 coated filter membrane and reach the endothelial monolayer. Under coculture conditions with H441 on the upper-side of the filter membrane and apical

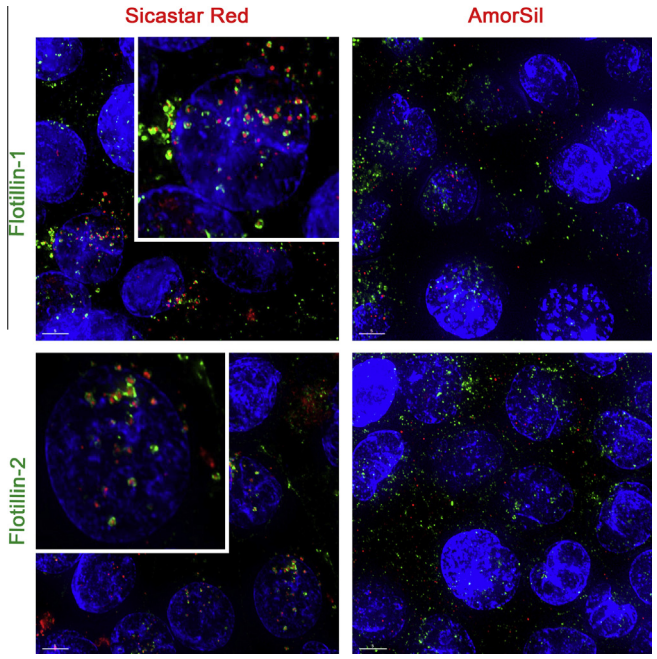

Fig. 6. Uptake studies of IF-stained H441 kept in coculture with ISO-HAS-1 exposed to Sicastar Red (60 μg/ml, red signal) and AmOrSil (300 μg/ml, red signal) for 4 h and further 20 h cultivation). H441 were counterstained for flotillin-1 and flotillin-2 (green signal). A clear incorporation of Sicastar Red in flotillin-1 and -2 containing vesicles could be detected. No colocalisation could be observed for AmOrSil. Nuclei are stained using Hoechst 33342 (blue), scale bar: 5 μm.

exposure of NPs, no uptake could be observed in ISO-HAS-1 for both NPs (Fig. 7, right column), although a detectable uptake was seen after 48 h exposure on the apical side of the filter membrane.

3.10. Evaluation of the barrier properties after NP exposure to the coculture via transepithelial electrical resistance TER

The barrier properties were also evaluated following the apical (H441) exposure to Sicastar Red and AmOrSil. TER (Fig. 8A) was measured after exposure to Sicastar Red (60–300 μg/ml) for 4 h and 4 h/20 h (4 h exposure and 20 h further cultivation in fresh serum-containing medium). Very high concentrations (300 μg/ml) resulted in a dramatic decrease of TER after 4 h (11.5 ± 6.6% of t_0) and remained significant reduced during the 20 h recovery period (24 ± 21% of t_0). Furthermore, TER was also checked for the permanent incubation for 48 h to Sicastar Red (60 μg/ml) and AmOrSil (300 μg/ml). No significant alterations to the TER occurred during the 48 h exposure compared to the untreated control, which demonstrated that a functional barrier was present during coculture transport experiments. The untreated control showed reduced TER values after 24 h (91 ± 8% of t_0), and these further decreased after 48 h (76 ± 11% of t_0). But, even with the reduction of TER, a functional barrier could be maintained after 48 h with 390 ± 83 Ω cm^2.

3.11. Inflammatory responses of the coculture after NP treatment

IL-8 and sICAM released from cells was determined after Sicastar Red exposure for 4 h/20 h (60–300 μg/ml). As control groups, transwell-monocultures (H441, seeded on the top and ISO-HAS-1

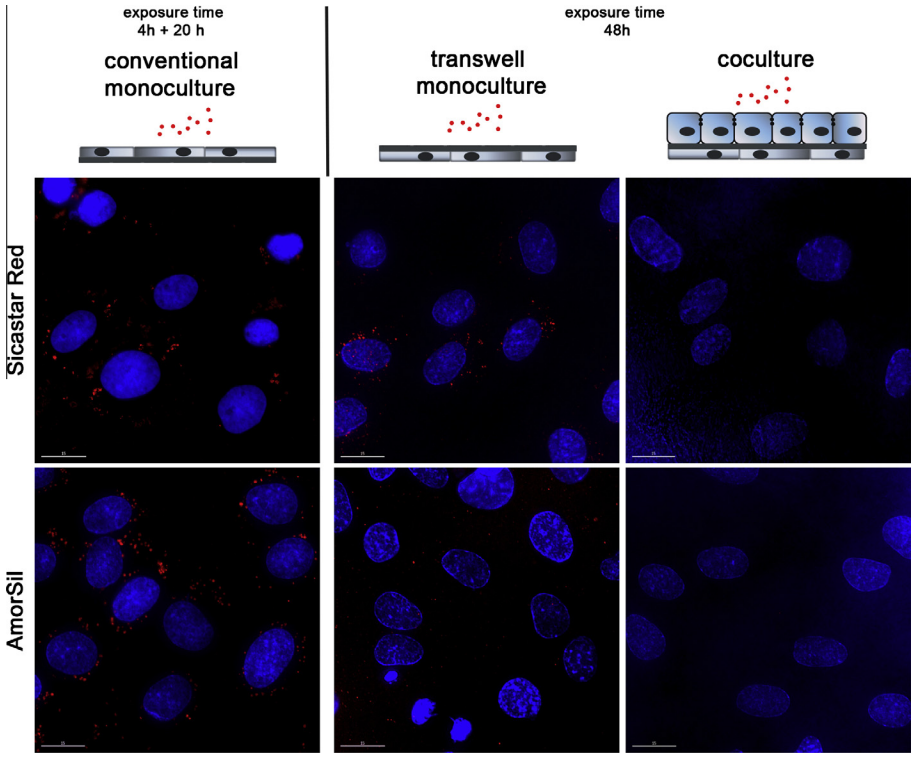

Fig. 7. Evaluation of the uptake of apically applied NPs (Sicastar Red: 60 μg/ml), AmOrSil: 300 μg/ml) in ISO-HAS-1 cells using different exposure conditions. Left column: ISOHAS-1 under conventional monoculture conditions (Incubation for 4 h with 20 h further cultivation in fresh medium, Sicastar Red: 6 μg/ml, AmorSil: 300 μg/ml), middle and right column: ISO-HAS-1 under different coculture conditions (Incubation time: 48 h, Sicastar Red: 60 μg/ml, AmorSil: 300 μg/ml, middle column: ISO-HAS-1 as monoculture under coculture conditions, right column: ISO-HAS-1 in coculture with H441). Images were taken by means of a fluorescent microscope (DeltaVision, Applied Precision). Nuclei are stained using Hoechst 33342 (blue), scale bar: 10 μm.

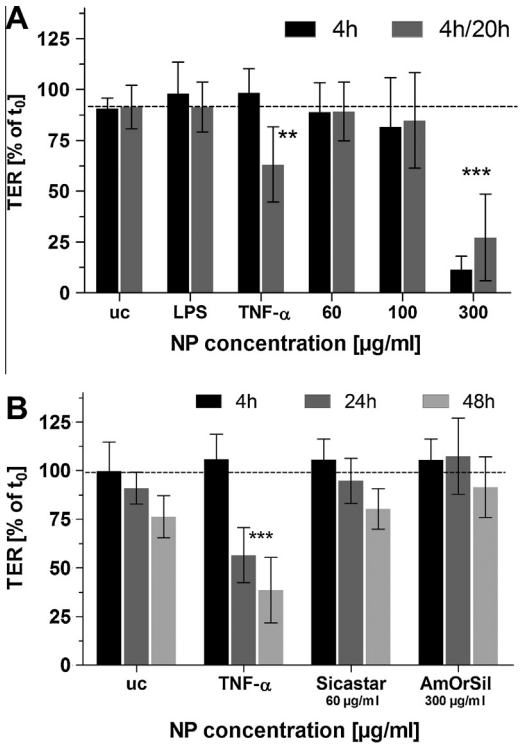

Fig. 8. Transepithelial electrical resistance (TER) of the coculture H441/ISO-HAS-1 was measured after (A) Sicastar Red exposure (60–300 µg/ml) for 4 h and 4 h with further 20 h cultivation in serum-containing medium without NPs and (B) 48 h permanent exposure of Sicastar Red (60 µg/ml) and AmOrSil. TER values are depicted as % of time-point t_0 (TER value prior to NP treatment). Results are shown as means ± SD of three independent experiments with $n = 3$ samples for each treatment. For statistical analysis one-way ANOVA with Dunnett's Multiple Analysing test was chosen. $^{*}P < 0.05$, $^{**}P < 0.01$ and $^{***}P < 0.001$ compared to the untreated control.

seeded on the bottom side of the filter membrane) were evaluated along with the coculture under the same culture conditions with Sicastar Red applied apically (on the H441 side). A concentration of 300 µg/ml in the CC resulted in a dramatic IL-8 release into the upper compartment (27 ± 9-fold of untreated control uc) but not into the lower compartment, which was on the contrary observed for the H441 transwell-monoculture without ISO-HAS-1 in the lower chamber (4 ± 1.2-fold of uc). However, a significant increase of sICAM (1.76 ± 0.4% of uc) could be detected in the lower compartment of the CC (ISO-HAS-1 side) after exposure to 300 µg/ml Sicastar Red. The monoculture with ISO-HAS-1 showed higher levels of sICAM (60 µg/ml: 2.25 ± 1.3%, 100 µg/ml: 2.3 ± 0.6%, 300 µg/ml: 3.3 ± 1.1% of uc) in the apical (upper) compartment (the stimulated side and basolateral side of the ISO-HAS-1). A concentration of 60 µg/ml Sicastar Red did not cause an IL-8 elevation after 4 h/20 h but after 48 h continuous exposure (7.5 ± 3.5% of uc).

4. Discussion

4.1. Cytotoxicity

In this paper, we first examined the cytotoxicity of NP in MC and CC to determine on the one hand the nontoxic concentrations of NPs but also the concentration ranges that allowed the microscopic detection of the particle uptake in the mono- and cocultures or epithelial and endothelial cells, respectively. For the uptake in MC lower concentrations of Sicastar Red particles (6 µg/ml) showed no toxic effects on epithelial cells, and an uptake in cells was detectable by fluorescence microscopy. In contrast, we observed a lower sensitivity of cells to Sicastar particles in the CC as indicated by the absence of toxic effects at concentrations of 60 µg/ml, which were also sufficient to detect NP uptake in the CCs. The results examining cytotoxicity (MTS and LDH) and inflammatory responses (IL-8 and sICAM) of NP-exposed H441 and ISO-HAS-1 in MC show dose-dependent cytotoxic effects for Sicastar Red, especially at higher concentrations such as 100 and 300 µg/ml. However, for AmOrSil, no harmful effects could be observed at all end-points.

According to the data for general cytotoxicity and inflammatory activation cells used in this model appeared to tolerate the AmOrSil particles, even though these were present in higher mass concentrations than the Sicastar particles. At the concentrations used, Sicastar always provided a much larger surface compared to AmOrSil in regard to the smaller particle size, which may also explain its higher toxicity. However, a direct comparison of the cytotoxicity of the two different silica-based particles should not merely base on their mass concentration due to their different size, mass and particle density. Thus, using the same administered mass of the NPs leads on the one hand to a different applied particle number and particle surface area and on the other hand it may lead to different cellular doses (compared to the administered dose on the cells) due to different particokinetics (diffusion, gravitational settling, agglomeration) of the particles [16]. In addition, different endocytotic pathways, that NPs may follow, might lead to differential toxicological effects. Beside size and shape, the cytotoxic effect of silica nanoparticles can primarily be associated to the reactivity of the nanoparticle surface which interfaces with the biological milieu. As reviewed by Napierska et. al., the hydrophilicity which is due to surface silanol groups is linked to cellular toxicity [1]. Since Sicastar Red is a hydrophilic amorphous silica nanoparticle with a plain/unfunctionalized surface it exerted a higher cytotoxicity. No obvious toxicity was observed for the organically modified and hydrophobic poly(organosiloxane) particle AmOrSil, whose silanol groups are mostly condensed into siloxane bonds. Furthermore, AmOrSil is coated with poly(ethylene oxide) (PEO) to achieve a water-solubility. Coating of NPs with poly(ethylene glycol) (PEG) or as in our case poly(ethylene oxide) (PEO) is widely applied in research concerning nanoparticles generated for biomedical applications. Suh and co-workers [2] reported that PEGylation improved the stability of NPs in aqueous solutions, gave a more efficient and constant crossing of NPs through biological obstacles and an improved cytoplasmic transport after endosomal escape, suggesting a reduction of nonspecific adhesion to cytoskeletal elements.

4.2. Cellular uptake routes

To determine cellular entry mechanisms of nanoparticles, current research is focussing on endocytotic pathways such as clathrin-mediated and caveolae-mediated endocytosis. Recent studies emphasise certain NP characteristics, such as size, shape and surface properties, that may be crucial in determining or allowing entry into respective pathways [17]. In addition, uptake mechanisms may depend on cell and differentiation specific endocytose mechanisms, and this may result in significant differences when comparing cells from different sources or states of differentiation.

Silica-based NPs have been widely applied in nanobiomedicine research as drug/gene vehicles (Reviewed by Kunzmann et. al. [1]). Poly(organosiloxane) core–shell nanoparticles are also being examined for prospective biomedical applications. AmOrSil NPs has a magnetic core, giving the prospect of novel therapeutic applications. Magnetic NPs are already used for biomedical applications, such as hyperthermia, magnetic resonance imaging and drug delivery [10,11].

Colocalisation studies using Sicastar Red and AmOrSil revealed no classical uptake mechanisms (clathrin-mediated and caveolae-mediated, see Fig. 2). Within the time points chosen in this study, none of the NPs colocalised either with markers for clathrin-mediated endocytosis (e.g. clathrin heavy chain: chc) or with markers for caveolin-dependent pathways (e.g. Caveolin-1: cav). Even short exposure times (5 min) could not reveal a colocalisation with clathrin-coated vesicles which have a lifetime of a few seconds, before they shed the clathrin and recycle it to the plasma membrane. Those static colocalisation experiments may not detect such transient events properly and they should be supported by e.g. inhibition experiments. Several recent studies indeed suggested clathrin-mediated uptake of silica-based particles such as unmodified mesoporous silica [18,19], which is a different type of silica material, containing ordered nanoscale pores (whereas Sicastar is unporous). Glebov et. al. studied endocytosis mechanisms involving clathrin-, caveolae-, as well as flotillin-dependent pathways by applying several inhibition methods for these distinct endocytosis mechanisms [20]. Our recent study using flotillin-1 and -2 depleted (siRNA transfection) H441 cells accentuated a contribution of flotillins in cellular uptake mechanisms of silica nanoparticles, since the uptake of NPs was reduced in flotillin-1/2 depleted cells [21].

In our previous study, we compared, besides cytotoxicity and inflammation, cellular uptake of aSNPs of different sizes (30, 70 and 300 nm in diameter), whereas all sizes were clearly incorporated in flotillin-1 and flotillin-2 labelled vesicles of H441 and ISO-HAS-1 in MC [21]. This study also demonstrates an incorporation of Sicastar Red and AmOrSil in flotillin-1- or flotillin-2-labelled vesicles, thus indicating an involvement of flotillin-1/2, at least in trafficking or in storage mechanisms (Fig. 3). Flotillin-1 and flotillin-2 (also called reggie-2 and reggie-1, respectively) are lipid raft-associated proteins and are thought to be involved in clathrin- and caveolae-independent endocytosis pathways, which is already stated by several studies [22–25]. Another study discussed a contribution of flotillins to maturation processes of late phagosomes in macrophages (J774) [26]. Furthermore, Vercauteren and coworkers reported a flotillin-1-dependent uptake mechanism of polyplexes in retinal pigment epithelium (RPE) cells [27]. These results corroborate the findings demonstrated in the present study, in which flotillin-1/2 were partially detected in LAMP-1-bearing vesicles of H441 and ISO-HAS-1 (see additional Fig. 1), but it did not colocalize with early endosomal marker proteins such as EEA1 (early antigen 1, data not shown).

Since this phenomenon occurs in a variety of cell types such as macrophages (J774), epithelial cells (H441, HeLa, RPE) or endothelial cells (ISO-HAS-1), it appears to be a general phenomenon. Thus, flotillins may play a general key role in late- or lysosomal degradation or storage processes.

Uptake experiments with Sicastar and AmOrSil in H441 which were carried out under coculture conditions also revealed an incorporation in flotillin-1 and -2 labelled vesicles for Sicastar Red but not for AmOrSil (Fig. 6) after an incubation period of 4 h and 20 h further cultivation in fresh serum-containing media. The H441 cells in coculture differed from the monoculture with respect to time-and dose-dependency of the nanoparticle uptake.

4.3. Quantification of NP uptake in H441 in mono- and coculture

Quantification experiments clearly showed NPs to a higher extent in H441 in MC compared to H441 in CC with ISO-HAS-1. Based on fluorescence intensity measurements, the H441 in CC did not take up the NPs (Fig. 5A and B). The polarised, barrier-forming H441 in CC required an increased exposure time (permanent 48 h) and an up to 10x higher dose than MCs to observe a visible uptake of Sicastar Red.

The reasons for these observations are currently unclear but might be associated to the more restrictive barrier in the CC or with more matured endocytosis mechanisms. The H441 in CC with ISO-HAS-1 displayed a barrier-forming cell phenotype with a more differentiated and polarised state similar to that observed in the *in vivo* biological barrier. These cells develop a tight barrier demonstrated by a continuous circumferential ZO-1 (zonula occludens-1) staining [9,28]. The H441/ISO-HAS-1 coculture achieve a transepithelial electrical resistance (TER) value that averages 560 ± 6 Ω cm^2 [9,28]. Furthermore, H441 cells in coculture develop a differentiated apical (as well as basolateral) membrane with a distinct setup of membrane components as well as microvilli [15], which are typical for ATII cells *in vivo* and may compromise NP uptake also.

This may also explain why AmOrSil did not colocalize with flotillins in H441 in coculture indicating a slower or narrowed uptake behaviour in the coculture. The uptake for AmOrSil could not be detected with higher incubation times or concentrations (Fig. 5C). This may lead to the conclusion that this material is likely to be inert in the lung *in vivo*. Whether differences of NP uptake in MC or CC occur seems to depend also on the nanoparticle properties as already mentioned in the cytotoxicity section. These inert properties are giving the prospect of a well-controlled and targeted uptake when further specific modifications are conducted to target a distinct uptake route or site or even a cell type (e.g. alveolar macrophages).

Hermanns et al. [28] described comparable uptake results for PEI (poly(ethyleneimine)) in MC compared to the H441 in CC. In addition, our recent study showed that the cells maintained under coculture conditions displayed a higher resistance upon aSNP exposure as monitored by membrane integrity (LDH assay) and an increased sensitivity based on the inflammatory responses (sICAM, IL6 and IL-8) [9]. This indicates that the amount of NPs taken up, which was dramatically reduced in the coculture compared to the conventional monoculture, correlates with the cytotoxic effects.

A comparison of the nanoparticle uptake behaviour of epithelial (H441) and endothelial cells (ISO-HAS-1) would also be very interesting, since endothelial cells differ from epithelial cells in regard to their physiological function, and reflected in differences in morphology, membrane composition and the less restrictive barrier compared to epithelial cells. Unfortunately, quantification via fluorescence intensity measurements is not possible due to the different cellular properties, which are mentioned above. This might lead to a putative different agglomeration behaviour of internalised NPs, which leads to an altered fluorescence light scattering and therewith to unprecise measurements. A more precise quantification method would be with ICP-AES (Inductively Coupled Plasma-Atomic Emission Spectrometry) which has previously been shown to be a unique and precise method [29,30] to quantify and compare gold nanoparticle uptake in epithelial and endothelial cells. Nevertheless, in MCs colocalisation of NPs with flotillin-1/2 was observed as soon as 4 h after exposure in ISO-HAS-1, indicating a faster uptake mechanism compared to H441, which showed a colocalisation first after 4 h/20 h (data not shown). Since cellular uptake as well as transcytosis or transport processes of molecules via membrane vesicles or caveolae are a hallmark of endothelial cells, this might explain the faster uptake compared to the epithelial cells (H441) [31].

4.4. Transport across the barrier

According to the transport studies of NPs across the lung barrier model, the NP-exposed epithelial layer displayed a functional barrier *in vitro* that prevented a direct passage through the transwell. According to the TER measurement during the transport experiment, the NPs did not affect the barrier properties significantly which verifies a functional *in vitro* barrier during the entire incubation period for 48 h (Fig. 8B). The slight reduction in TER after 48 h,

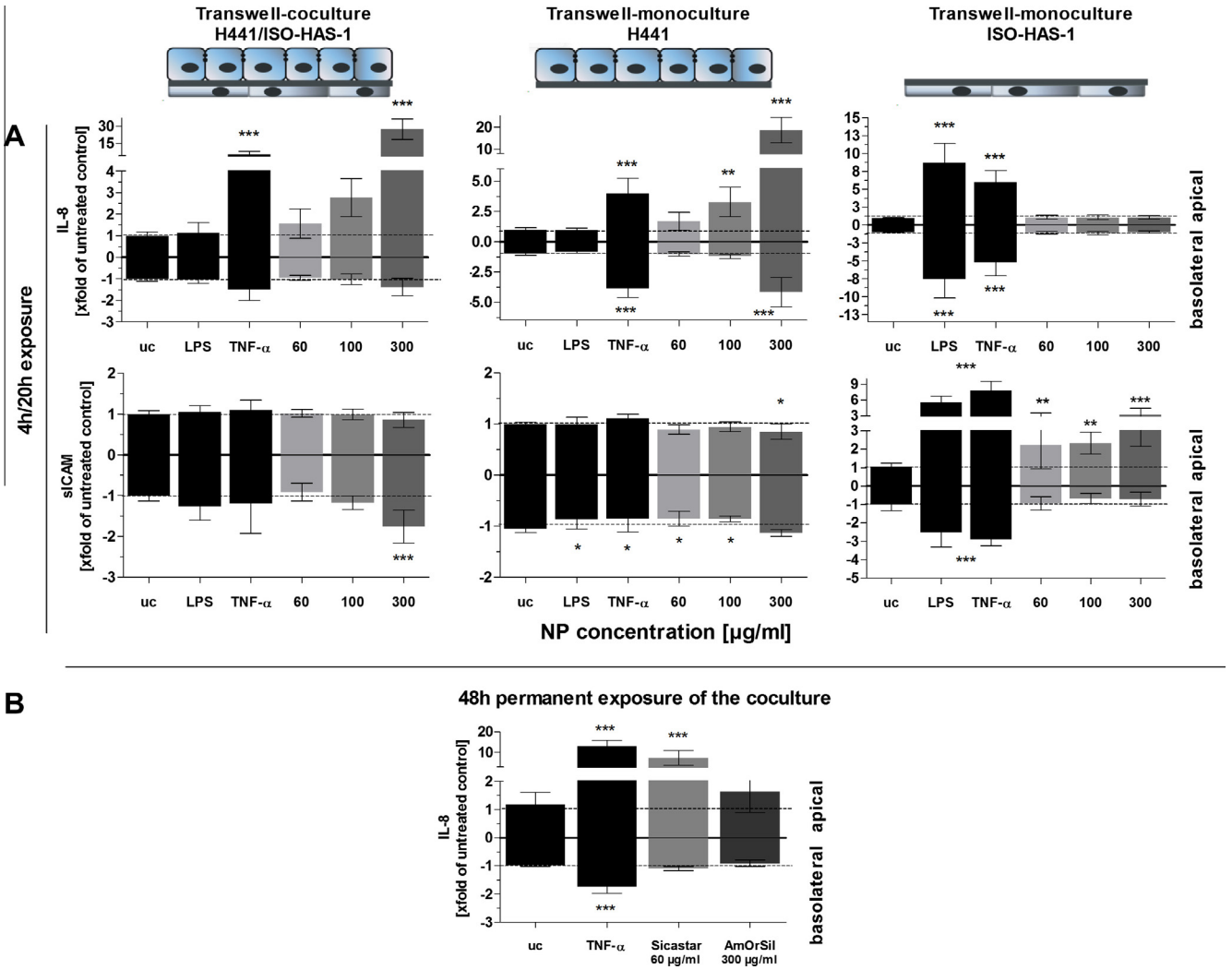

Fig. 9. The release of inflammatory mediators (IL-8, sICAM) is shown after NP exposure to apical/basolateral differentiated cocultures of H441 and ISO-HAS-1, as well as their appropriate monocultures grown on HTS 24-Transwell® filters. Cells were exposed to NPs from the apical side of the filter membrane to mimic an inhalative exposure. (A) After 4 h serum-free incubation of the cocultere with Sicastar Red (60–300 µg/ml), NPs were removed and the cells were cultivated for further 20 h in serum-containing medium without NPs. (B) IL-8 measurement after 48 h permanent exposure of the coculture to Sicastar Red (60 µg/ml) and AmOrSil (300 µg/ml). After NP treatment (A and B), supernatant of both compartments (apical: upper well, basolateral: lower well) was examined. Uc: untreated control, LPS (1 µg/ml), TNF-α (300 U/ml). Data are depicted as means (*x*-fold of untreated control uc) ± SD of three independent experiments with $n = 3$. For statistical analysis two-way ANOVA with Bonferronie's post test was conducted. $^{*}P < 0.05$, $^{**}P < 0.01$ and $^{***}P < 0.001$ compared to the untreated control. (For interpretation of the references to colour in this figure legend, the reader is referred to the web version of this article.)

which was also observed for the untreated control, might be due to the cultivation in low serum (2.5%). This compromise has been done to avoid on the one hand nanoparticle agglomeration due to serum and on the other hand to minimise TER interferences due to the absence of serum. But, even with the reduction in TER a functional barrier could be maintained after 48 h with 390 ± 83 Ω cm^2. However, a comparison of the short term exposure without serum and the long-term exposure with low serum is limited by the fact that particles may display an altered uptake behaviour as well as cytotoxicity and inflammatory potential of the SNPs due to the particle protein corona as it is mentioned in recent studies [32,33].

4.5. Inflammation

In this study, an exposure of the coculture to Sicastar Red (60 µg/ml) resulted in elevated IL-8 levels in the upper compartment (H441 side) after 48 h but not in the lower compartment (Fig. 9B), whereas the incubation for 4 h with further recovery period for 20 h in serum-containing medium without Sicastar Red did not show an IL-8 release (Fig. 9A). This indicates the relevance of also using longer incubation times to evaluate cellular effects of NPs. Dose-dependent inflammatory responses of the coculture was also affirmed for Sicastar Red (60–300 µg/ml) at an incubation time of 4 h with further 20 h recovery in serum-containing medium without NPs. At a concentration of 300 µg/ml, the coculture showed a significant IL-8 release in the upper compartment (H441) but not in the lower compartment, whereas the H441 transwell-monoculture showed a release in both the upper and lower well. Additionally, the TER values were dramatically reduced at this high concentration in both the coculture and H441 transwell-monoculture to a similar extent. This indicated that the IL-8 originating from the epithelial cells did not cross the endothelial layer even with a disrupted epithelial barrier. The fact that a concentration of 300 µg/ml in the coculture resulted in a sICAM release on the endothelial side but not on the epithelial side may indicate cross-talk between IL-8 (among others) releasing H441 and endothelial cells, which were consequently triggered to release sICAM. Beside leucocyte adhesion and transmigration, sICAM is considered to play a role in cardiovascular disease progression

[34] and thus may be assumed as a crucial mediator concerning the indirect extrapulmonary effects caused by NPs. According to visual judgments, both epithelial and endothelial monolayers were sustained after incubation with a concentration of 300 μg/ml Sicastar Red. This also may explain the fact that an apical (H441) increase of IL-8 with increasing Sicastar concentrations was detectable in CC, however the H441 in MC responded with a decrease of IL8 with increasing Sicastar concentrations which is due to a severe cell loss. Conversely, an increased sICAM release was observed for H441 in MC, whereas no sICAM response was detectable for H441 in CC. This might be due to a higher differentiation and polarisation of the H441 considering a well-developed apical membrane with microvilli concluding an altered shedding of adhesion molecules.

Furthermore, an increased uptake (compared to a concentration of 60 μg/ml, as used for the transport experiments) was observed for the direct exposed H441 but not in the ISO-HAS-1 on the bottom side in which no fluorescence signals of NPs could be detected. These findings corroborate the above mentioned conclusion. These results also corroborate the observation by Kasper et al. [9], which described cross-talk between direct aSNP-exposed H441 with ISO-HAS-1 resulting in an inflammatory response of the endothelial layer, which did not have a direct contact to NPs. A reason for the endothelial sICAM release may also be due to the elevated LDH release of the H441 and reduced TER. These finding could be attributed to the presence of necrotic cells at these very high concentrations. LDH, ATP and other cytosolic components, which are released by necrotic cells, are known to cause inflammation. The induction of inflammatory processes induced by cell damage play also a significant role in the development of acute lung injury (ALI) or obstructive lung diseases (COPD). High concentrations such as 300 μg/ml used in this study probably exceed concentrations of NPs which may occur during inhalation processes *in vivo*, but they serve very well as a positive control for the *in vitro* setting. In consequence, subsequent approaches would have to take into account effects caused by long-term or repeated exposure to nanoparticle in lower doses as it may occur in the development of obstructive lung diseases.

5. Conclusion

According to this study, flotillins appear to play a role in cellular uptake or trafficking mechanisms of NPs and are discussed as indicators for clathrin- or caveolae-independent uptake mechanisms. Furthermore, the coculture model H441/ISO-HAS-1 represents a suitable model to study nanoparticle interactions with the alveolar epithelial barrier *in vitro*. It allows an investigation into cellular uptake/transport of nanoparticles as well as cell–cell communication processes after nanoparticle exposure at the alveolar-capillary site. In addition to an induction and release of inflammatory signals after NP exposure, which causes local effects on cells of the alveolar barrier, this study proposes forwarded inflammatory signals which may provoke further systemic effects. We are currently investigating a primary cell coculture model of the alveolar-capillary barrier consisting of primary human ATII (alveolar type II cells) and HPMEC (human pulmonary microvascular endothelial cells) to compare these cells to the model described in these studies. The primary ATII differentiate into ATI cells after 7–10 days of cultivation [35] and give the opportunity to study nanoparticle interactions with alveolar type-I cells.

Acknowledgements

A portion of the work described herein was carried out by Jennifer Kasper in partial fulfilment of the requirements for a biological doctoral degree at the Johannes Gutenberg University, Mainz, Germany.

The authors wish to thank Ms. Elke Hübsch and Ms Michaela Moisch for their excellent assistance with the cell culture and immunocytochemical studies. This study was supported by the DFG priority program SPP 1313 within the Cluster BIONEERS and also by the European Union, FP6 Project NanoBioPharmaceutics.

Appendix A. Supplementary material

Supplementary data associated with this article can be found, in the online version, at http://dx.doi.org/10.1016/j.ejpb.2012.10.011.

References

[1] A. Kunzmann, B. Andersson, T. Thurnherr, H. Krug, A. Scheynius, B. Fadeel, Toxicology of engineered nanomaterials: focus on biocompatibility, biodistribution and biodegradation, Biochim. Biophys. Acta 2011 (1810) 361–373.
[2] D. Napierska, L.C. Thomassen, D. Lison, J.A. Martens, P.H. Hoet, The nanosilica hazard: another variable entity, Part Fibre Toxicol. 7 (2010) 39.
[3] A. Nemmar, P.H. Hoet, B. Vanquickenborne, D. Dinsdale, M. Thomeer, M.F. Hoylaerts, H. Vanbilloen, L. Mortelmans, B. Nemery, Passage of inhaled particles into the blood circulation in humans, Circulation 105 (2002) 411–414.
[4] J. Schwartz, Air pollution and hospital admissions for heart disease in eight U.S. counties, Epidemiology 10 (1999) 17–22.
[5] J.D. Poloniecki, R.W. Atkinson, A.P. de Leon, H.R. Anderson, Daily time series for cardiovascular hospital admissions and previous day's air pollution in London, UK, Occupat. Environ. Med. 54 (1997) 535–540.
[6] N.L. Mills, N. Amin, S.D. Robinson, A. Anand, J. Davies, D. Patel, J.M. de la Fuente, F.R. Cassee, N.A. Boon, W. MacNee, A.M. Millar, K. Donaldson, D.E. Newby, Do inhaled carbon nanoparticles translocate directly into the circulation in humans?, Am J. Respir. Crit. Care Med. 173 (2006) 426–431.
[7] A. Nemmar, B. Nemery, M.F. Hoylaerts, J. Vermylen, Air pollution and thrombosis: an experimental approach, Pathophysiol. Haemost. Thromb. 32 (2002) 349–350.
[8] M.I. Hermanns, J. Kasper, P. Dubruel, C. Pohl, C. Uboldi, V. Vermeersch, S. Fuchs, R.E. Unger, C.J. Kirkpatrick, An impaired alveolar-capillary barrier in vitro: effect of proinflammatory cytokines and consequences on nanocarrier interaction, J. Roy. Soc. Interface 7 (Suppl. 1) (2010) S41–S54.
[9] J. Kasper, M.I. Hermanns, C. Bantz, M. Maskos, R. Stauber, C. Pohl, R.E. Unger, J.C. Kirkpatrick, Inflammatory and cytotoxic responses of an alveolar-capillary coculture model to silica nanoparticles: comparison with conventional monocultures, Part Fibre Toxicol. 8 (2011) 6.
[10] S. Utech, C. Scherer, M. Maskos, Multifunctional, multicompartment polyorganosiloxane magnetic nanoparticles for biomedical applications, J. Magn. Magn. Mater. 321 (2009) 1386–1388.
[11] S. Utech, C. Scherer, K. Krohne, L. Carrella, E. Rentschler, T. Gasi, V. Ksenofontov, C. Felser, M. Maskos, Magnetic polyorganosiloxane core-shell nanoparticles: synthesis, characterization and magnetic fractionation, J. Magn. Magn. Mater. 322 (2010) 3519–3526.
[12] T.J. micromod Partikeltechnologie GmbH, Grüttner, C. Rudershausen. S, Westphal, F. Verfahren zur Herstellung gefärbter und fluoreszenter Polykieselsäure-Partikel, in: E.P. Office (Ed.), Germany, 2000.
[13] M. Masuzawa, T. Fujimura, Y. Hamada, Y. Fujita, H. Hara, S. Nishiyama, K. Katsuoka, H. Tamauchi, Y. Sakurai, Establishment of a human hemangiosarcoma cell line (ISO-HAS), Int. J. Cancer 81 (1999) 305–308.
[14] R.E. Unger, V. Krump-Konvalinkova, K. Peters, C.J. Kirkpatrick, In vitro expression of the endothelial phenotype: comparative study of primary isolated cells and cell lines, including the novel cell line HPMEC-ST1.6R, Microvasc. Res. 64 (2002) 384–397.
[15] M.I. Hermanns, R.E. Unger, K. Kehe, K. Peters, C.J. Kirkpatrick, Lung epithelial cell lines in coculture with human pulmonary microvascular endothelial cells: development of an alveolo-capillary barrier in vitro, Lab. Invest. 84 (2004) 736–752.
[16] J.G. Teeguarden, P.M. Hinderliter, G. Orr, B.D. Thrall, J.G. Pounds, Particokinetics in vitro: dosimetry considerations for in vitro nanoparticle toxicity assessments, Toxicol. Sci. 95 (2007) 300–312.
[17] J.L. Vivero-Escoto, B.G. Trewyn, V.S. Lin, Mesoporous silica nanoparticles for intracellular controlled drug delivery, Small 6 (2010) 1952–1967.
[18] D.M. Huang, Y. Hung, B.S. Ko, S.C. Hsu, W.H. Chen, C.L. Chien, C.P. Tsai, C.T. Kuo, J.C. Kang, C.S. Yang, C.Y. Mou, Y.C. Chen, Highly efficient cellular labeling of mesoporous nanoparticles in human mesenchymal stem cells: implication for stem cell tracking, FASEB J. 19 (2005) 2014–2016.
[19] T.H. Chung, S.H. Wu, M. Yao, C.W. Lu, Y.S. Lin, Y. Hung, C.Y. Mou, Y.C. Chen, D.M. Huang, The effect of surface charge on the uptake and biological function of mesoporous silica nanoparticles in 3T3-L1 cells and human mesenchymal stem cells, Biomaterials 28 (2007) 2959–2966.

[20] H. Damke, T. Baba, A.M. van der Bliek, S.L. Schmid, Clathrin-independent pinocytosis is induced in cells overexpressing a temperature-sensitive mutant of dynamin, J. Cell Biol. 131 (1995) 69–80.
[21] J. Kasper, M.I. Hermanns, C. Bantz, O. Koshkina, T. Lang, M. Maskos, C. Pohl, R.E. Unger, J.C. Kirkpatrick, Interactions of silica nanoparticles with lung epithelial cells and the association to flotillins, Arch. Toxicol. (2012).
[22] I.C. Morrow, S. Rea, S. Martin, I.A. Prior, R. Prohaska, J.F. Hancock, D.E. James, R.G. Parton, Flotillin-1/reggie-2 traffics to surface raft domains via a novel golgi-independent pathway. Identification of a novel membrane targeting domain and a role for palmitoylation, J. Biol. Chem. 277 (2002) 48834–48841.
[23] O.O. Glebov, N.A. Bright, B.J. Nichols, Flotillin-1 defines a clathrin-independent endocytic pathway in mammalian cells, Nat. Cell Biol. 8 (2006) 46–54.
[24] T. Ait-Slimane, R. Galmes, G. Trugnan, M. Maurice, Basolateral internalization of GPI-anchored proteins occurs via a clathrin-independent flotillin-dependent pathway in polarized hepatic cells, Mol. Biol. Cell 20 (2009) 3792–3800.
[25] M.F. Langhorst, A. Reuter, F.A. Jaeger, F.M. Wippich, G. Luxenhofer, H. Plattner, C.A. Stuermer, Trafficking of the microdomain scaffolding protein reggie-1/flotillin-2, Eur. J. Cell Biol. 87 (2008) 211–226.
[26] J.F. Dermine, S. Duclos, J. Garin, F. St-Louis, S. Rea, R.G. Parton, M. Desjardins, Flotillin-1-enriched lipid raft domains accumulate on maturing phagosomes, J. Biol. Chem. 276 (2001) 18507–18512.
[27] D. Vercauteren, M. Piest, L.J. van der Aa, M. Al Soraj, A.T. Jones, J.F. Engbersen, S.C. De Smedt, K. Braeckmans, Flotillin-dependent endocytosis and a phagocytosis-like mechanism for cellular internalization of disulfide-based poly(amido amine)/DNA polyplexes, Biomaterials 32 (2011) 3072–3084.
[28] M.I. Hermanns, J. Kasper, P. Dubruel, C. Pohl, C. Uboldi, V. Vermeersch, S. Fuchs, R.E. Unger, C.J. Kirkpatrick, An impaired alveolar-capillary barrier in vitro: effect of proinflammatory cytokines and consequences on nanocarrier interaction, J. Roy. Soc. Interface 7 (Suppl. 1) (2010) S41–54.
[29] C. Freese, M.I. Gibson, H.A. Klok, R.E. Unger, C.J. Kirkpatrick, Size- and coating-dependent uptake of polymer-coated gold nanoparticles in primary human dermal microvascular endothelial cells, Biomacromolecules 13 (2012) 1533–1543.
[30] C. Freese, C. Uboldi, M.I. Gibson, R.E. Unger, B.B. Weksler, I.A. Romero, P.O. Couraud, C.J. Kirkpatrick, Uptake and cytotoxicity of citrate-coated gold nanospheres: comparative studies on human endothelial and epithelial cells, Part. Fibre Toxicol. 9 (2012) 23.
[31] S.A. Predescu, D.N. Predescu, A.B. Malik, Molecular determinants of endothelial transcytosis and their role in endothelial permeability, Am. J. Physiol. Lung Cell. Mol. Physiol. 293 (2007) L823–842.
[32] A. Panas, C. Marquardt, O. Nalcaci, H. Bockhorn, W. Baumann, H.R. Paur, S. Mulhopt, S. Diabate, C. Weiss, Screening of different metal oxide nanoparticles reveals selective toxicity and inflammatory potential of silica nanoparticles in lung epithelial cells and macrophages, Nanotoxicology (2012).
[33] A. Lesniak, F. Fenaroli, M.P. Monopoli, C. Aberg, K.A. Dawson, A. Salvati, Effects of the presence or absence of a protein corona on silica nanoparticle uptake and impact on cells, ACS Nano 6 (2012) 5845–5857.
[34] N.S. Jenny, A.M. Arnold, L.H. Kuller, A.R. Sharrett, L.P. Fried, B.M. Psaty, R.P. Tracy, Soluble intracellular adhesion molecule-1 is associated with cardiovascular disease risk and mortality in older adults, J. Thromb. Haemost. 4 (2006) 107–113.
[35] M.I. Hermanns, S. Fuchs, M. Bock, K. Wenzel, E. Mayer, K. Kehe, F. Bittinger, C.J. Kirkpatrick, Primary human coculture model of alveolo-capillary unit to study mechanisms of injury to peripheral lung, Cell Tissue Res. 336 (2009) 91–105.